

Pile response and free field vibrations due to low strain dynamic loading

Masoumi, H.R. & Degrande, G.

Department of Civil Engineering, K.U. Leuven, Kasteelpark Arenberg 40, B-3001 Leuven, Belgium

Holeyman, A.

Department of Civil Engineering, Université Catholique de Louvain, B-1348 Louvain-la-Neuve, Belgium

Keywords: low strain dynamic testing, impact pile driving, pile response, ground vibrations

ABSTRACT: This paper presents the results of in situ measurements during dynamic pile testing at a construction site in Louvain-la-Neuve. Main objectives are the investigation of the pile response and the free field vibrations due to low strain dynamic loading on a single cast-in-situ pile with a 5 kg hammer impact on the pile head. Whereas low strain testing is usually performed to assess the integrity of the pile as a structural member, this study focuses on both pile and ground vibrations. The pile head response and ground motions are measured with accelerometers during different blows with the impact hammer. The dynamic characteristics of the soil are determined with a SASW test. Experimental results are compared with predictions obtained with a coupled finite element-boundary element model. The computed pile head and free field response show a good correspondence with the measured response. In addition, the static stiffness of the pile estimated by means of the mobility function shows a very good agreement with the value calculated by an analytical formulation.

1 INTRODUCTION

In an urban environment, vibrations generated by construction activities such as pile driving, blasting and dynamic compaction often affect surrounding buildings. Many case histories demonstrate that vibrations are not only disturbing for people, but also cause settlement of structures (Kim and Lee, 2000; Athanasopoulos and Pelekis, 2000). Because of the importance of pile driving in engineering construction and its environmental effects, the study of the ground vibrations due to pile driving and their effects on structures has received considerable attention during the last two decades (Woods and Sharma, 2004; Dowding, 1996). Pre-construction surveying, monitoring and control of vibrations, and prediction of anticipated vibrations, are important steps to prevent intolerable effects.

A literature review shows that there is a general lack of information concerning the environmental impact of ground vibrations due to pile driving. Studies have mostly focused on monitoring of the pile integrity (low strain testing) (Seidel, 2000; Rausche et al., 1992; Holeyman, 1992) and on the assessment of the static and dynamic bearing capacity of piles (high strain testing) (Holeyman, 1992; Middendorp and van Brederode, 1985; Likins et al., 2000).

Complementary numerical models are required to obtain a deeper understanding of the pile response and the wave transmission in the free field. A few contributions have been focusing on the prediction

of the transmission of vibrations into the free field for vibratory and impact pile driving (Ramshaw et al., 1998; Al-Abdeh, 2005).

Very recently, Masoumi et al. (2007) have proposed a linear coupled finite element-boundary element (FE-BE) model to predict vibrations in the free field due to vibratory and impact pile driving. The model is based on a subdomain formulation for dynamic soil-structure interaction where the pile is modelled using the finite element method and the soil is modelled using the boundary element method. An extension of this model to account for the non-linear constitutive behaviour of the soil in the immediate vicinity of the pile has also been developed (Masoumi et al., 2007).

In order to obtain a better understanding of the pile and soil response during pile driving and to validate results of the numerical model developed by Masoumi et al. (2007), in-situ measurements using low strain dynamic testing have been performed at a construction site at Anneau Central in Louvain-la-Neuve (Belgium). The pile response and free field vibrations at different distances from the pile are investigated due to a low impact with a 5 kg instrumented hammer on a single pile (i.e. dynamic low strain testing). This impact induces elastic waves which are transmitted through the pile and the surrounding soil with low energy and a relatively high frequency content.

In practice, low strain testing is commonly used to assess the construction quality of cast in-situ piles. The most complete low strain dynamic tests, referred to as the mechanical impedance test or the transient dynamic

response test, involve the impact of the pile head by a hand-held hammer and monitoring the impact force and the pile head response (Seidel, 2000; Holeyman, 1992). Holeyman (1992) has presented a state-of-the-art of technological aspects of dynamic pile testing including test methods, loading equipment, data acquisition and interpretation.

This paper is organised as follows. The test site is discussed in section 2. Next, the experimental setup, as well as representative experimental results are presented in section 3. The time history and frequency content of the measured and predicted pile head response as well as the ground vibrations at different distances from the pile are compared in section 4. Finally, the mobility or transfer function between the impact force and the response is assessed, together with the corresponding coherence function, and compared with numerical predictions.

2 SITE DESCRIPTION

The construction site is located at Anneau Central in Louvain-La-Neuve (Belgium). At this site, a university library is constructed on piled raft foundations with a total of 120 piles (Figure 1).

The 0.46 m diameter reinforced concrete piles have been installed using pressure casting. Two piles P7 and P15 are selected for low strain testing and equipped with a casing extension. Pile P7 has a total length of 9.85 m with an embedment depth of 8.55 m. Pile P15 has a total length of 7.32 m with an embedment depth of 6.02 m. Laboratory tests performed on concrete samples (taken during pile installation) result in a Young's modulus varying between 31500 and 36500 MPa for the piles at the time of testing (Tomboy and Holeyman, 2006).

The soil consists of a homogeneous layer of Brussels sand. A SASW test has been performed to determine the dynamic soil characteristics. The SASW method is a non-intrusive geophysical prospection method for the determination of the shear wave velocity C_s of the top layers as a function of the depth z . Surface waves generated by a hammer impact on a small rigid foundation are recorded at different distances from the source. An inversion procedure is used to minimize the difference between the experimental and the theoretical dispersion curve (Nazarian and Desai, 1993).

The inversion procedure is performed for a dry sand with a Poisson's ratio of $\nu = 0.33$ and a density of $\rho = 1900 \text{ kg/m}^3$. The SASW test results in a soil medium consisting of a shallow layer with a thickness of 0.55 m and a shear wave velocity $C_s = 108 \text{ m/s}$ and a stiffer layer with a thickness of 1.8 m and a shear wave velocity $C_s = 168 \text{ m/s}$ on top of a half space with a shear wave velocity $C_s = 258 \text{ m/s}$ (Geraedts et al., 2005). No detailed information on the material damping ratio in the different layers could be obtained from the surface wave test results. In section 4, numerical results will therefore be presented for two values of the material damping ratio β_s , which are typical for shallow layers of sandy soil: $\beta_s = 0.01$ and $\beta_s = 0.025$. It is assumed that the material damping ratio is the same for volumetric and deviatoric deformation and uniform with depth.

3 LOW STRAIN DYNAMIC TESTING

3.1 Experimental configuration

Figure 1 shows an overview of the two measurement setups used for the excitation on pile P7 (setup 1) and

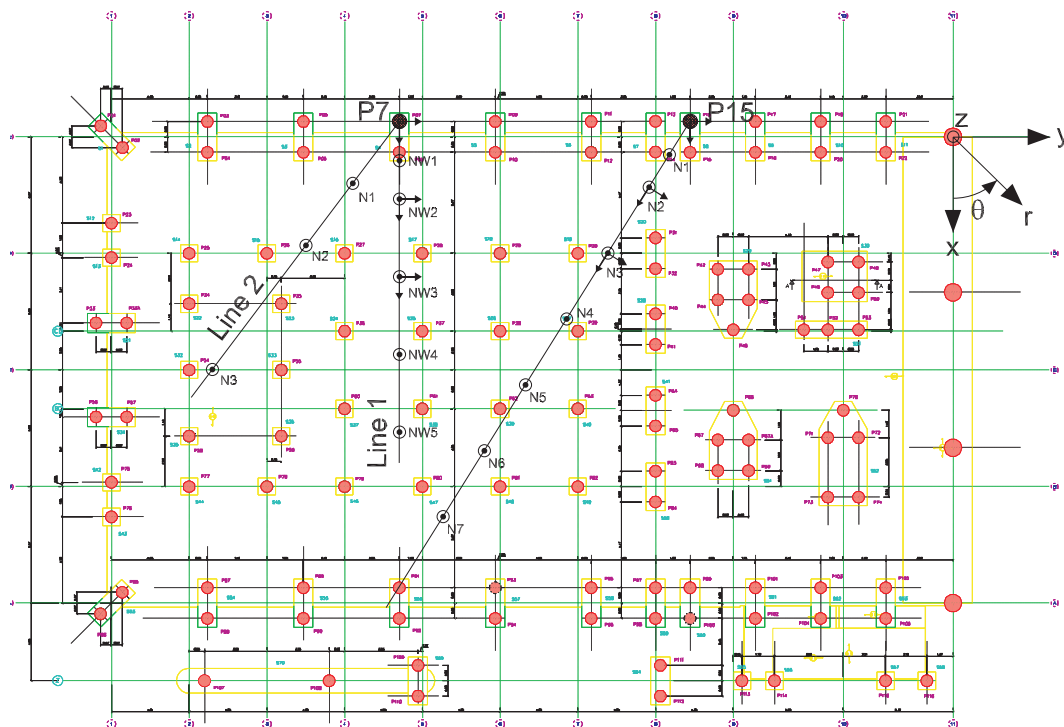


Figure 1. An overview of the measurement setup 1 (excitation on pile P7) and setup 2 (excitation on pile P15) on the construction site in Louvain-la-Neuve.

on pile P15 (setup 2), respectively. In both setups, use is made of one force sensor, 15 accelerometers, a KEMO VBF35 unit and a 16 bit Daqbook 216 data-acquisition system, coupled to a portable PC (Masoumi et al., 2006). The vertical accelerations in the free field are measured with seismic PCB accelerometers, mounted on an aluminium stake with a cruciform cross section to minimize dynamic soil-structure interaction.

In setup 1, the accelerometers are located along the measurement line 1 at distances from 2 up to 16 m from the pile P7 and along the measurement line 2 at distances from 4 to 16 m from the pile P7. In setup 2, the accelerometers are located along a single measurement line at distances from 2 to 24 m from pile P15.

Hand-held hammers for low strain dynamic testing typically have a mass from 0.5 to 5 kg and produce an impact force in the range from 5 to 5000 N. In the present test, a large hammer with a mass $m = 5.5$ kg and a soft tip has been used to impact the pile head.

3.2 Measurement results

In setup 1, a total of 11 hammer blows have been applied on the pile P7. The time history of the force, the acceleration at the pile head and the free field acceleration are investigated. As the time histories for all blows are very similar, only results for the first blow are discussed in the following. The average of all blows is considered, however, to estimate the transfer function between the applied force and the free field velocity (or the mobility) and the corresponding coherence functions.

As the present study mainly focuses on the response in the free field, all signals have been low-pass filtered using analog filters with a cut-off frequency at 250 Hz for the impact force and at 125 Hz for the accelerations at the pile and in the free field (Masoumi et al., 2006). This low-pass filtering affects the measured response at the pile head, but does not have a major influence on the free field response.

Figure 2 shows the time history and the frequency content of the impact force due to the first blow on the pile P7. An impulsive force is generated with a maximum value of about 7 kN. The frequency content of the force is affected by the low-pass filtering at 250 Hz.

Figure 3 shows the time history of the accelerations in the free field along measurement line 1 as a function of the distance from the center of pile P7 due to blow number 1. Since all traces are scaled with respect to their maximum value, this figure does not allow to appreciate the vibration attenuation with the distance from the source. The first trace at a distance $r = 0$ m represents the pile head response.

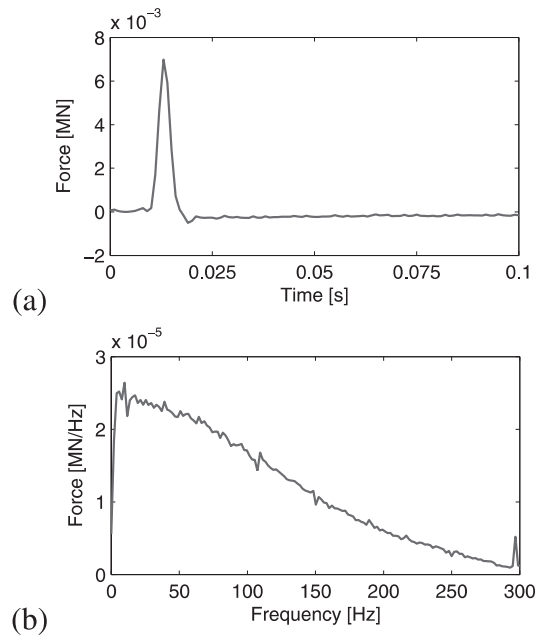


Figure 2. (a) Time history and (b) frequency content of the impact force on the pile P7 (setup 1, event 1).

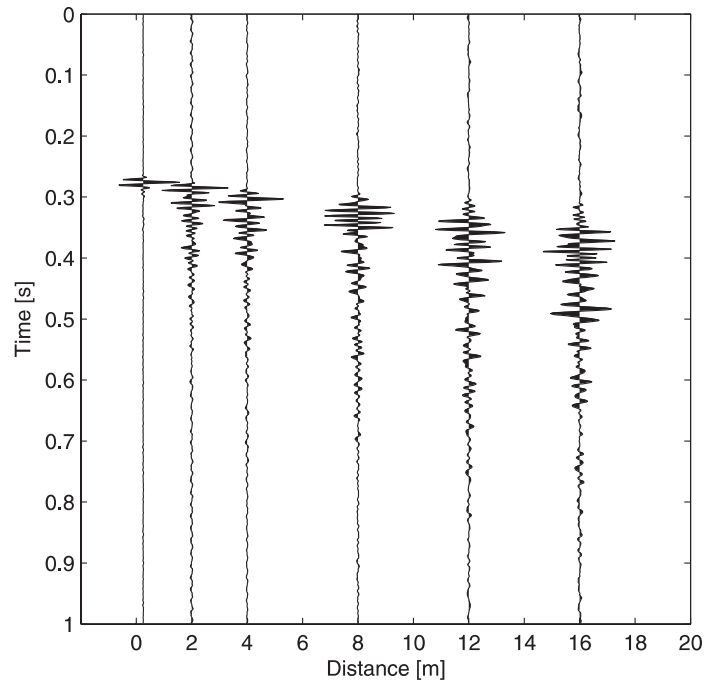


Figure 3. Time history of the accelerations in the free field along measurement line 1 as a function of the distance from the center of the pile P7 (setup 1, event 1).

4 EXPERIMENTAL AND NUMERICAL RESULTS

The experimental results are compared with the predictions computed with the numerical model developed by Masoumi et al. (2007). Predictions are made for the impact force measured during the first blow in setup 1 (Figure 2).

In the numerical model, the pile has a Young's modulus $E_p = 36000$ MPa, a Poisson's ratio $\nu_p = 0.25$, and a density $\rho_p = 2500$ kg/m³. The longitudinal wave velocity of the pile is equal to $C_{lp} = 3800$ m/s. The pile is partially embedded ($e_p = 8.55$ m) in the soil medium (Figure 4).

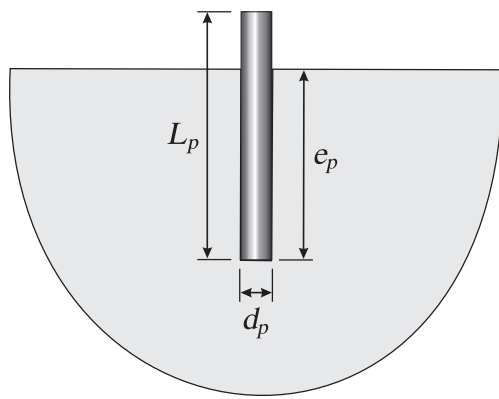


Figure 4. Geometry of an embedded pile in a soil medium.

The layered soil medium consists of a shallow layer with a thickness of 0.55 m and a Young's modulus $E_s = 58.95$ MPa and a stiffer layer with a thickness of 1.8 m and a Young's modulus $E_s = 142.6$ MPa on top of a half space with a Young's modulus $E_s = 336.4$ MPa. A constant Poisson's ratio $\nu_s = 0.33$ and density $\rho_s = 1900$ kg/m³ are assumed along the depth. In addition, it is also assumed that material damping in the soil can be represented by a constant material damping ratio β_s in volumetric and deviatoric deformation. The material damping in the soil is accounted for by the correspondence principle through the use of a frequency independent complex shear modulus $\mu_s^* = \mu_s(1 + 2i\beta_s)$. No detailed information on the material damping ratio in the different layers could be obtained from the surface wave tests. Therefore, numerical results are presented for two values of the material damping ratio β_s , which are typical for shallow layers of sandy soil: $\beta_s = 0.01$ and $\beta_s = 0.025$.

Based on a dynamic soil-structure interaction formulation, a coupled finite element-boundary element model has been developed to predict free field vibrations due to pile driving (Masoumi et al., 2007). A linear elastic constitutive behaviour is assumed for the pile and the soil. The pile (bounded domain) is modelled using the finite element method and the soil is modeled by means of a boundary element formulation based on the Green's functions of a horizontally stratified soil. Using a modal decomposition technique, the equation of the coupled system is solved in the frequency domain and the response in the time domain is computed using the inverse Fourier transform (Masoumi and Degrande, 2008).

The pile is modeled using 8-node isoparametric brick elements. The size of these elements corresponds to the size of the boundary elements along the pile-soil interface, which is dictated by the minimum shear wavelength in the soil, as described below. As the pile has a cylindrical shape and the vertical kinematic impedance of the pile is investigated, only the axisymmetric modes consisting of the vertical rigid body mode and the flexible axial modes of the pile are considered. A convergence analysis has demonstrated that it is sufficient to

account for one rigid body mode and three axial modes of the pile with free boundary conditions in order to perform accurate predictions in the frequency range of interest, which is derived from the frequency content of the impact force (Masoumi et al., 2007).

The boundary element analysis is applied to compute the dynamic stiffness matrix of the soil. The size of the boundary elements on the soil-pile interface is limited to 0.05 m at the pile toe and 0.125 m along the pile shaft. The equation of motion of the coupled system is solved in the frequency domain and the response in the time domain is computed using the inverse Fourier transform. For comparison with the experimental results, predicted results are filtered with the same low-pass filter as the field measurements.

Figure 5 shows the time history and the frequency content of the vertical velocity of the pile head during the first impact (event 1) on the pile P7, obtained by numerical integration of the measured acceleration. The maximum vertical velocity at the pile head is equal to 1.8 mm/s. Figure 5 displays a very good agreement between the predicted and measured pile head velocity. As expected, the predicted pile head response only weakly depends on the material damping ratio in the soil.

Figure 6 shows the time history and the frequency content of the vertical velocity in the free field along the measurement line 1. The amplitude of the vertical velocity attenuates as the distance from the pile increases. The maximum particle velocity varies from 0.35 mm/s at $r = 2$ m to less than 0.1 mm/s at $r = 16$ m. The frequency content of the free field velocity is mainly dominated by frequencies in the range between 25 and 125 Hz in the near field and

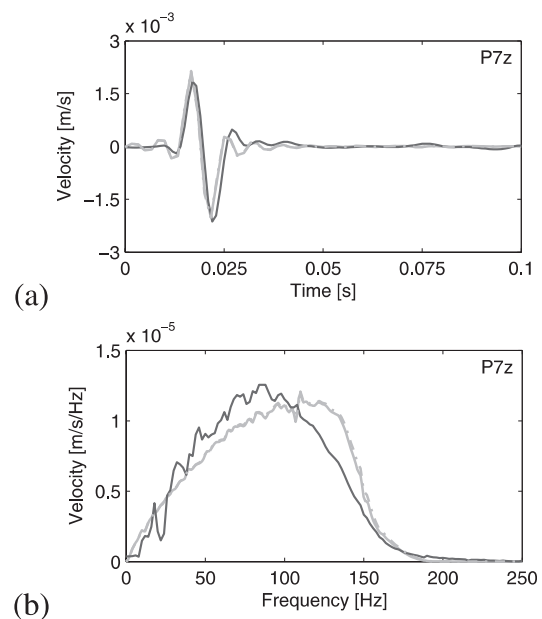


Figure 5. (a) Time history and (b) frequency content of the vertical velocity of the pile head P7 (setup 1, event 1) (black solid line), compared with the predicted response for a material damping ratio $\beta_s = 0.01$ (gray dash-dotted line) and $\beta_s = 0.025$ (gray solid line).

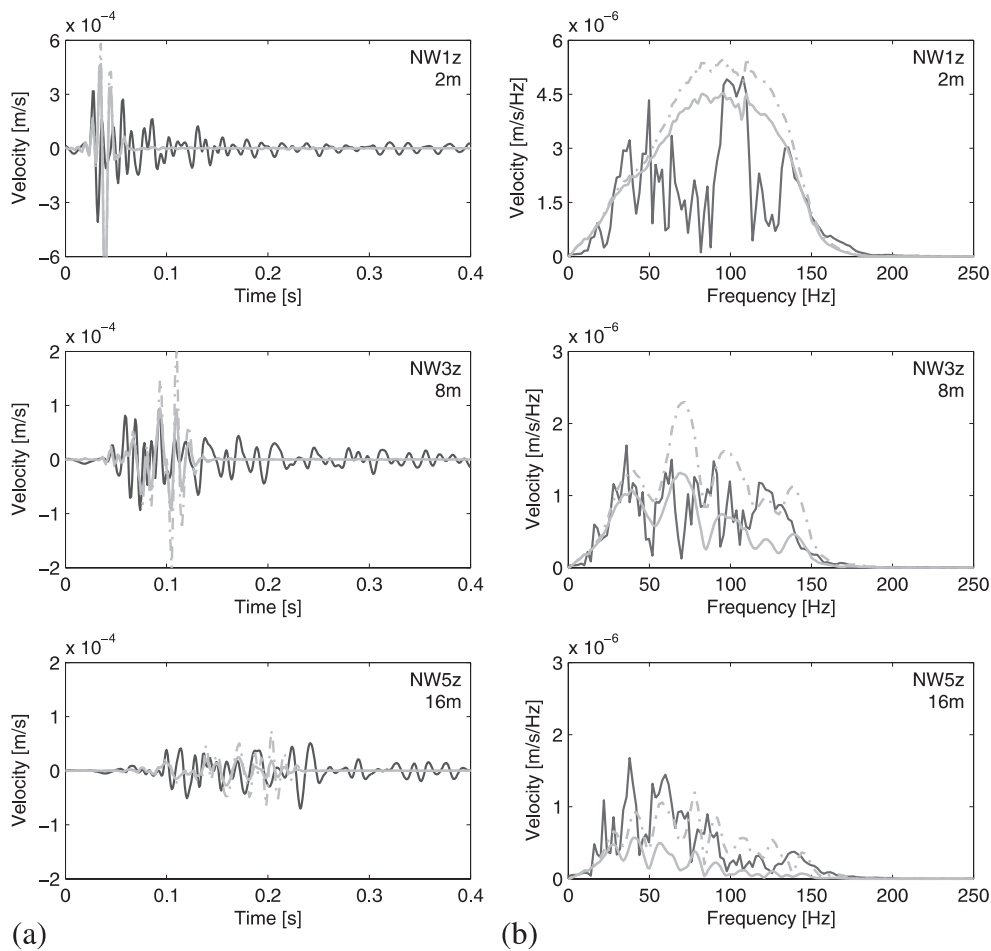


Figure 6. (a) Time history and (b) frequency content of the vertical velocity in the free field at different distances from the pile P7 along measurement line 1 (setup 1, event 1) (black solid line), compared with the predicted response for a material damping ratio $\beta_s = 0.01$ (gray dash-dotted line) and $\beta_s = 0.025$ (gray solid line).

between 25 and 100 Hz in the far field. The frequency content of the free field response shifts to lower frequencies for increasing distance to the source due to material damping.

In Figure 6, experimental results are also compared with the results of numerical predictions. Predicted vibrations show a reasonable correspondence with the measurements. At distance of 2 m from the pile, the predicted peak particle velocities (PPV) are respectively a factor 1.50 and 1.25 higher than the measured values, even for the highest value $\beta_s = 0.025$ of the material damping ratio. The frequency content of the predicted vibrations still shows a reasonable agreement with the measurements. It can also be observed that for points near the pile, the amplitude of the vibrations predicted with a material damping ratio $\beta_s = 0.025$ is in better correspondence with the measured data. As the distance from the pile increases, a better correspondence between the measured and predicted vibrations is obtained with a lower material damping ratio $\beta_s = 0.01$. This observation reveals that the material damping ratio may not be constant, but rather decreases with depth, as waves with longer wavelength seem to be less affected by material damping in the soil. Therefore, the determination of the variation of the material damping ratio of the soil with depth is

indispensable for an accurate prediction of the free field response.

Figure 7 displays the variation of the vertical PPV on the ground surface as a function of the distance from the pile P7 along measurement lines 1 and 2. Field measurements are compared with the envelope of predicted results for a material damping ratio $\beta_s = 0.01$ (upper bound) and $\beta_s = 0.025$ (lower bound). A reasonable agreement is found between the predicted and measured results in the far field ($r > 4$ m). In the near field, however, a significant

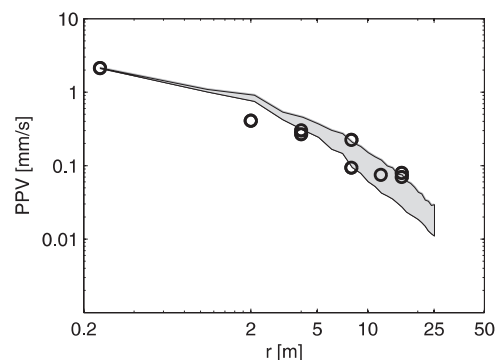


Figure 7. Vertical PPV on the ground surface (\circ) as a function of the distance from the pile P7 along measurement lines 1 and 2 (setup 1, event 1), compared with the envelope of the predicted PPV for a material damping ratio $\beta_s = 0.01$ (upper bound) and $\beta_s = 0.025$ (lower bound).

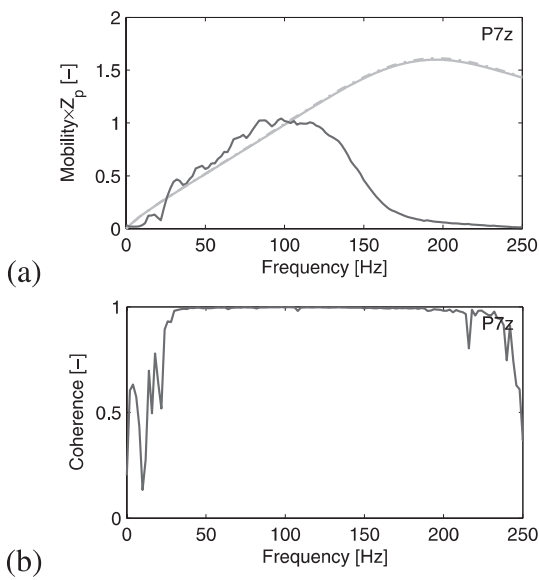


Figure 8. (a) Dimensionless vertical mobility and (b) coherence function at the pile P7 (setup 1, all events) (black solid line), compared with the predicted mobility for a material damping ratio $\beta_s = 0.01$ (gray dash-dotted line) and $\beta_s = 0.025$ (gray solid line).

discrepancy is observed: the experimental measurements show a smaller attenuation coefficient and the predictions are conservative, even with a material damping ratio $\beta_s = 0.025$.

Figure 8 shows the dimensionless mobility and corresponding coherence function at the pile head of the pile P7. Results are based on an average of all 11 events considered in setup 1. The coherence function is a measure for the statistical validity of the estimation of the transfer function (mobility) where a zero value indicates no causal relationship between the input and the output and a value of 1.0 indicates the existence of a linear noise-free relation between the input and the output. The coherence function is independently normalized at each frequency and is therefore independent of the shape of the frequency content of the recorded signals. Figure 8b displays low coherence values at low frequencies below 20 Hz and at high frequencies above 200 Hz. At low frequencies, this is due to the fact that the hammer impact does not provide a sufficiently large excitation. At frequencies between 30 and 175 Hz, however, the impact force and the response are coherent.

The mobility function in figure 8a is normalized by multiplication with the mechanical impedance $Z_p = \rho_p C_p A_p$ of the pile, where C_p denotes the longitudinal wave velocity in the pile and A_p is the cross sectional area of the pile. If the pile head mobility is linear in the range of low frequencies between 0 and 100 Hz, its slope s provides an estimation of the static flexibility of the pile

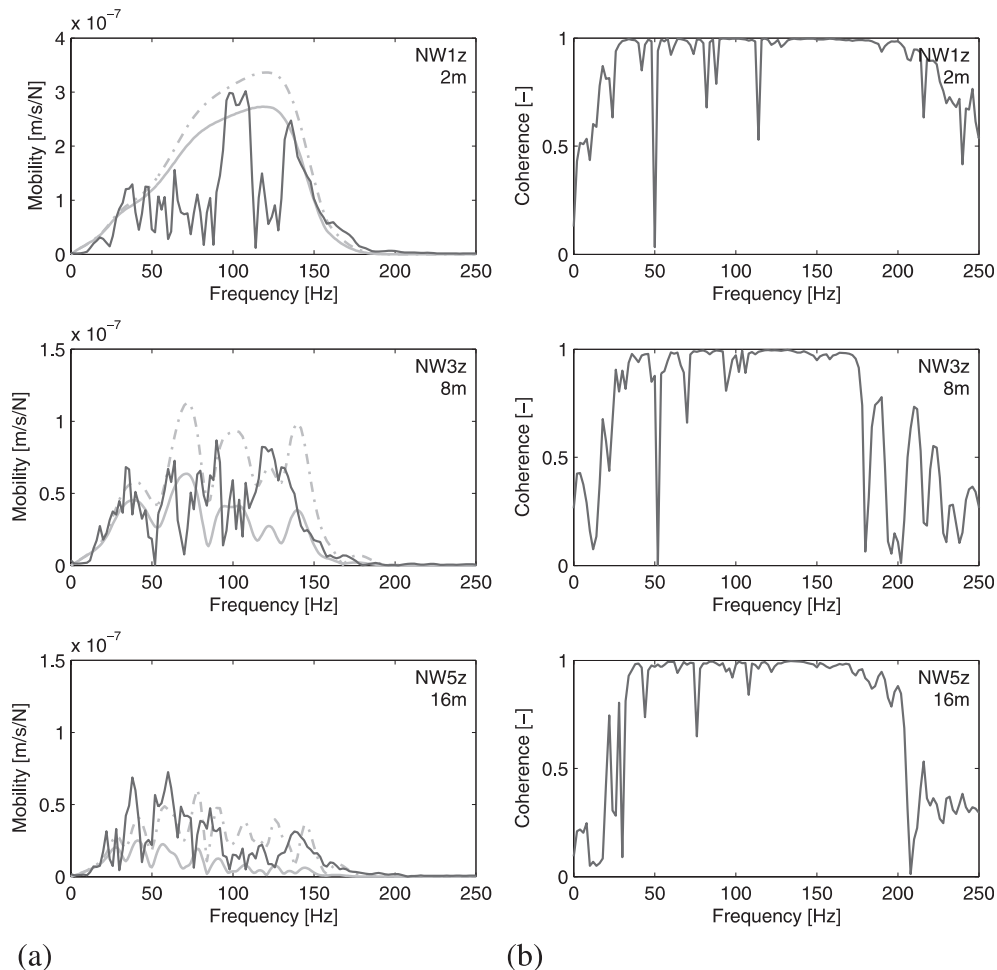


Figure 9. (a) Mobility and (b) coherence functions in the free field at different distances from the pile P7 along measurement line 1 (setup 1, all events) (black solid line), compared with the predicted mobility for a material damping ratio $\beta_s = 0.01$ (gray dash-dotted line) and $\beta_s = 0.025$ (gray solid line).

(Rausche et al., 1992): $s = \|\dot{u}/F\|/\omega \simeq 1.15 \times 10^{-3} \text{ m/MN}$. This value results in an estimated static stiffness of 869 MN/m. According to Kaynia and Kausel (Kaynia and Kausel, 1991), the vertical static stiffness of a single pile with $L_p/d_p = 20$ embedded in a homogeneous half space with $E_s = E_p/100$ is equal to $1.58E_pA_p/L_p = 918 \text{ MN/m}$. The static stiffness evaluated by means of the mobility function is close to this analytical value.

The predicted mobility also shows a constant slope at low frequencies. In figure 8a, the predicted pile head response is not low-pass filtered and results are presented for higher frequencies up to 300 Hz to better show the characteristics of the mobility function. At high frequencies or when the pile is infinitely long or highly damped at its toe, the mobility becomes constant and tends to $1/Z_p$, so that the expected normalised mobility is expected to tend to 1. A pile with less damping at the toe and no friction along the shaft is expected to have a larger mobility (Rausche et al., 1992) (a free pile has infinite mobility). At high frequencies, the predicted normalised mobility displayed in figure 8 has a higher average value around 1.4, corresponding to a mechanical impedance of the pile P7 around $0.7 Z_p$, which is lower than the impedance Z_p . The predicted mobility shows a maximum at the frequency $f_c = C_p/2L_p = 195 \text{ Hz}$ which corresponds to the first axial natural frequency of the pile. Since the measured pile head response is affected by low-pass filtering, no similar conclusions can be drawn from the measured average mobility in the high frequency range.

Figure 9 compares the experimental and predicted mobility in the free field at different distances from the pile P7 along measurement line 1. This figure also displays the coherence derived from the experimental results. Coherence values close to 1 are observed in the near field in the frequency range between 30 and 150 Hz. This frequency range reduces with increasing the distance from the pile due to material damping in the soil. At low frequencies, the Rayleigh wavelength is much larger than the thickness of the soft shallow layers and the mobility of the layered soil medium is mainly influenced by the characteristics of the underlying half space. At high frequencies and long distances from the pile, the mobility shows the behaviour of the soft top layers (Auersch, 1994). In the near field and at frequencies below 75 Hz, the predicted and the measured mobility show a reasonable correspondence. The sensitivity of the response to the material damping ratio in the soil is small. In the far field and at higher frequencies, however, the predicted mobility with $\beta_s = 0.01$ shows a better agreement with the measured mobility. An important discrepancy is observed at high frequencies. An accurate determination of the material damping ratio is therefore needed to obtain a better correspondence between the predicted and measured results.

5 CONCLUSIONS

A low strain dynamic test has been performed at a construction site in Louvain-la-Neuve (Belgium). The pile response as well as the free field vibrations due to a hammer impact on a single pile have been investigated. Experimental results have been compared with the results of numerical predictions, obtained with a coupled finite element-boundary element model, where the pile and the soil are modelled using the finite element method and the boundary element method, respectively.

The following conclusions can be drawn:

- The time history and the frequency content of the measured and predicted pile head response correspond well.
- Coherence functions of the recorded data show that the field measurements are well correlated to the impact force at frequencies between 30 Hz and the cut-off frequency. The coherence ratio at frequencies smaller than 30 Hz is less than 1, because the energy associated with the hammer impact is not large enough to overcome the toe and the shaft resistance.
- A reasonable agreement is found between the predicted and measured response in the far field ($r > 4 \text{ m}$). In the near field, however, a significant discrepancy is observed and the predictions are conservative even with a material damping ratio $\beta_s = 0.025$. The experimental results indeed show a smaller attenuation coefficient.
- At high frequencies and at long distances from the pile, results depend on the material damping ratio of the soil. Therefore, a careful determination of the material damping ratio of the soil is crucial for a successful prediction of free field vibrations.
- The static stiffness of the pile estimated by means of the mobility function shows a very good correspondence with the value calculated with an analytical formulation as well as with predicted values.
- The numerical model has been successfully validated by means of in-situ measurements. This model can be usefully applied to determine the pile and the free field response for those cases where low deformations in the soil are expected.

ACKNOWLEDGEMENTS

The results presented in this paper have been obtained within the frame of the SBO project IWT 03175 "Structural damage due to dynamic excitation: a multi-disciplinary approach". This project is funded by IWT Vlaanderen, the Institute of the Promotion of Innovation by Science and Technology in Flanders. Their financial support is gratefully acknowledged.

REFERENCES

- Al-Abdeh, R. (2005). *Étude des vibrations induites dans le sol par le battage et le vibrofonçage de pieux*. Ph. D. thesis, Université des Sciences et Technologies de Lille, France.
- Athanasopoulos, G. and Pelekis, P. (2000). Ground vibrations from sheetpile driving in urban environment: measurements, analysis and effects on buildings and occupants. *Soil Dynamics and Earthquake Engineering* 19, 371–387.
- Auersch, L. (1994). Wave propagation in layered soils: theoretical solution in wavenumber domain and experimental results of hammer and railway traffic excitation. *Journal of Sound and Vibration* 173(2), 233–264.
- Dowding, C. (1996). *Construction vibrations*. Englewood Cliffs, New Jersey: Prentice-Hall.
- Geraedts, K., Lombaert, G., Masoumi, H. and Degrande, G. (2005, July). Determination of the dynamic soil characteristics with the SASW method at a construction site in Louvain-la-Neuve. Report BWM-2005-07, Department of Civil Engineering, K.U. Leuven. SBO Project IWT 03175.
- Holeyman, A. (1992). Technology of pile dynamic testing. In F. Barends (Ed.), *Proceedings of the 4th International Conference on the Application of the Stress-Wave Theory to Piles*, The Hague, The Netherlands, pp. 195–215. A.A. Balkema, Rotterdam.
- Kaynia, A. and Kausel, E. (1991). Dynamics of piles and pile groups in layered soil media. *Soil Dynamics and Earthquake Engineering* 10(8), 386–401.
- Kim, D. and Lee, J. (2000). Propagation and attenuation characteristics of various ground vibrations. *Soil Dynamics and Earthquake Engineering* 19, 115–126.
- Likins, G., Rausche, F. and Goble, G. (2000). High strain dynamic pile testing equipment and practice. In S. Niyama and J. Beim (Eds.), *Proceedings of the 6th International Conference on the Application of the Stress-Wave Theory to Piles*, Sao Paulo, Brazil. A.A. Balkema, Rotterdam.
- Masoumi, H. and Degrande, G. (2008). Numerical modelling of free field vibrations due to pile driving using a dynamic soil-structure interaction formulation. *Journal of Computational and Applied Mathematics*. Special issue of ACOMEN 2005. In press.
- Masoumi, H., Degrande, G. and Lombaert, G. (2007). Prediction of free field vibrations due to pile driving using a dynamic soil-structure interaction formulation. *Soil Dynamics and Earthquake Engineering* 27(2), 126–143.
- Masoumi, H., Francois, S. and Degrande G. (2007, June). Numerical prediction of ground vibrations due to pile driving using a hybrid formulation. In K. Pitilakis (Ed.), *4th International Conference on Earthquake Geotechnical Engineering*, Thessaloniki, Greece.
- Masoumi, H., Lombaert, G. and Degrande G. (2006, November). Ground vibrations due to a hammer impact on a single pile at a construction site in Louvain-la-Neuve. Report BWM-2006-04, Department of Civil Engineering, K.U. Leuven. SBO Project IWT 03175.
- Middendorp, P. and van Brederode, P. (1985). Skin friction models for sand from static and dynamic laboratory load tests. In G. Holm, C. Gravare, and H. Bredenberg (Eds.), *Proceedings of the 2nd International Conference on the Application of the Stress-Wave Theory to Piles*, Stockholm, Sweden, pp. 210–221. A.A. Balkema, Rotterdam.
- Nazarian, S. and Desai, M. (1993). Automated surface wave method: field testing. *Journal of Geotechnical Engineering, Proceedings of the ASCE* 119(7), 1094–1111.
- Ramshaw, C., Selby, A. and Bettess, P. (1998). Computed ground waves due to piling. In P. Dakoulas, M. Yegian, and R. Holtz (Eds.), *Geotechnical Earthquake Engineering and Soil Dynamics III*, Seattle, pp. 1484–1495.
- Rausche, F., Likins, G. and Kung, S. (1992). Pile integrity testing and analysis. In F. Barends (Ed.), *Proceedings of the 4th International Conference on the Application of the Stress-Wave Theory to Piles*, The Hague, The Netherlands. A.A. Balkema, Rotterdam.
- Seidel, J. (2000). Presentation of low strain integrity testing in the time-frequency domain. In S. Niyama and J. Beim (Eds.), *Proceedings of the 6th International Conference on the Application of the Stress-Wave Theory to Piles*, Sao Paulo, Brazil. A.A. Balkema, Rotterdam.
- Tomboy, O. and Holeyman, A. (2006, February). Dynamic loading tests on a single pile in Louvain-la-Neuve. Technical report, Université Catholique de Louvain.
- Woods, R. and Sharma, V. (2004). *Dynamic effects of pile installations on adjacent structures*. London, UK: A.A. Balkema.